ANTIMICROBIAL AGENTS AND CHEMOTHERAPY, May 1994, p. 1052–1058
0066-4804/94/$04.00+0

Vol. 38, No. 5

# Biofilm Accumulation Model That Predicts Antibiotic Resistance of *Pseudomonas aeruginosa* Biofilms

PHILIP S. STEWART*

*Center for Biofilm Engineering and Department of Chemical Engineering, Montana State University, Bozeman, Montana 59717-0398*

Received 4 October 1993/Returned for modification 5 January 1994/Accepted 27 February 1994

**A computer model of biofilm dynamics was adapted to incorporate the activity of an antimicrobial agent on bacterial biofilm. The model was used to evaluate the plausibility of two mechanisms of biofilm antibiotic resistance by qualitative comparison with data from a well-characterized experimental system (H. Anwar, J. L. Strap, and J. W. Costerton, Antimicrob. Agents Chemother. 36:1208–1214, 1992). The two mechanisms involved either depletion of the antibiotic by reaction with biomass or physiological resistance due to reduced bacterial growth rates in the biofilm. Both mechanisms predicted the experimentally observed resistance of 7-day-old *Pseudomonas aeruginosa* biofilms compared with that of 2-day-old ones. A version of the model that incorporated growth rate-dependent killing predicted reduced susceptibility of thicker biofilms because oxygen was exhausted within these biofilms, leading to very slow growth in part of the biofilm. A version of the model that incorporated a destructive reaction of the antibiotic with biomass likewise accounted for the relative resistance of thicker biofilms. Resistance in this latter case was due to depletion of the antibiotic in the bulk fluid rather than development of a gradient in the antibiotic concentration within the biofilm. The modeling results predicted differences between the two cases, such as in the survival profiles within the biofilm, that could permit these resistance mechanisms to be experimentally distinguished.**

It is widely recognized that bacteria colonizing a surface as a biofilm can be much more resistant to antimicrobial chemotherapy than are their planktonic counterparts (4, 14). The reduced susceptibility of attached bacteria becomes crucial in the treatment of infections such as those associated with medical implants or cystic fibrosis (4). Two leading hypotheses have been advanced to explain the persistence of biofilm infections. The first hypothesis relates to antibiotic transport. According to this hypothesis, antimicrobial agents fail to fully penetrate the biofilm, so that in some regions of the biofilm, bacteria simply are not exposed to effective concentrations of an antibiotic (4, 10). The second explanation postulates that physiological differences of sessile cells, for example, low growth rates, reduce the susceptibility of microorganisms in the biofilm mode of growth (3, 8).

Both the transport-related and the physiological explanations for biofilm resistance to antibiotics have experimental support, suggesting that both mechanisms may operate to various degrees in real systems. Indeed, part of the difficulty in interpreting experimental results is that the same transport limitations that might prevent an antibiotic from penetrating a biofilm can very readily lead to physiological gradients within the biofilm. One way to distinguish the unique features of the two hypotheses is through theoretical investigation. This article introduces the use of a computer model of biofilm dynamics as a tool to augment laboratory work aimed at understanding the persistence of biofilm infections.

This article presents a theoretical evaluation of the plausibility of the transport limitation and altered physiology mechanisms of biofilm resistance to antimicrobial agents. The evaluation involves the comparison of predictions of a mathematical model of biofilm accumulation, which are customized to incorporate either of the two resistance mechanisms, with data from a well-characterized experimental system (1). The purpose of this investigation was to assess whether either mechanism, when analyzed quantitatively in terms of its constituent phenomena, could capture the qualitative behavior of the experimental data. A second objective was to discover differences between the predicted behaviors of the two mechanisms that might allow them to be experimentally discriminated.

## MATERIALS AND METHODS

An existing computer model of biofilm dynamics (9) was adapted to describe the activity of an antimicrobial agent on biofilm. This model was developed by researchers at the Center for Biofilm Engineering on the basis of the conceptual and mathematical formulation described by Wanner and Gujer (25). Its central principle is conservation of mass, which is applied to two compartments: bulk liquid and biofilm. The equations for the bulk liquid compartment simulate the dynamics of a chemostat, e.g., a well-mixed, constant-volume, continuous-flow reactor. Coupled to the equations describing bulk liquid constituents are separate balance equations pertaining to transport and reaction processes within the biofilm. The biofilm is treated as a uniformly thick planar aggregate whose composition changes only in the direction perpendicular to the substratum. This conceptual view of the biofilm permits a one-dimensional mathematical model. The full mathematical formulation of the model is listed in the Appendix. The following paragraphs give an overview of the basic model structure.

The biofilm model applied in this investigation incorporated processes of bulk flow in and out of the reactor, diffusion of dissolved species within the biofilm, substrate consumption by bacterial metabolism, bacterial growth, advection of cell mass within the biofilm, cell detachment from the biofilm, and antibiotic killing. Advection refers to the displacement of cells

* Mailing address: Center for Biofilm Engineering and Department of Chemical Engineering, Montana State University, 409 Cobleigh Hall, Bozeman, MT 59717-0398. Phone: (406) 994-2890. Fax: (406) 994-6098.

TABLE 1. Parameter values for biofilm modeling

| Parameter | Symbol | Value | Source or reference |
|---|---|---|---|
| Maximum specific growth rate | $\mu_{max}$ | 0.30 $h^{-1}$ | 11 |
| Oxygen yield coefficient | $Y_{xo}$ | 0.24 g $g^{-1}$ | 18 and 24 |
| Oxygen Monod coefficient | $K_o$ | 0.1 mg $liter^{-1}$ | 12 |
| Cell volume fraction | $\varepsilon_c$ | 0.10 | 6 |
| Cell intrinsic density | $\rho_x$ | 47,000 mg $liter^{-1}$ | 6, 17, and 20 |
| Initial biofilm thickness | $L_f^o$ | 1.39 μm | 1 |
| Oxygen bulk fluid concentration | $C_o^*$ | 0.035 mg $liter^{-1}$ | Fit |
| Antibiotic bulk fluid concentration | $C_a^*$ | 505 mg $liter^{-1}$ | 1 |
| Oxygen diffusion coefficient | $D_o$ | 0.090 $cm^2$ $h^{-1}$ | 16 |
| Antibiotic diffusion coefficient | $D_a$ | 0.020 $cm^2$ $h^{-1}$ | 16 |
| Biofilm-bulk diffusivity ratio | $\tau$ | 0.9 | 26 |
| Detachment rate coefficient | $k_d$ | 1 $cm^{-1}$ $h^{-1}$ | Fit |
| Surface area-to-volume ratio | $A/V$ | 592 $m^{-1}$ | 1 |
| Dilution rate | $Q/V$ | 0.125 $h^{-1}$ | 1 |
| Antibiotic kill rate (no reaction) | $k_a$ | 0.029 liter $mg^{-1}$ | Fit |
| Antibiotic kill rate (with reaction) | $k_a$ | 0.0385 liter $mg^{-1}$ $h^{-1}$ | Fit |
| Antibiotic reaction rate | $k_r$ | 0.0016 liter $mg^{-1}$ $h^{-1}$ | Fit |

away from the substratum due to the growth of their neighbors. Two particulate species were considered; these were conceptualized as live and dead cells. Both cell types occupied the same volume; however, only live cells metabolized substrate and were capable of growth. Two dissolved species, oxygen and antibiotic, were considered in the model. Oxygen was assumed to be the limiting substrate for microbial growth, as it is in most aerobic biofilm processes (2). The growth of live cells and concomitant consumption of oxygen was approximated by a Monod-type rate expression. The sole mechanism of transport of oxygen and antibiotic within the biofilm was molecular diffusion, modeled according to Fick's first law. The model allowed for a reduction in the effective diffusion coefficient inside the biofilm due to interference by particulate biofilm constituents. Resistance to mass transfer between the biofilm and the bulk fluid was neglected. The growth of live cells in the biofilm created new biomass volume that caused the biofilm to expand. At any point within the biofilm, the advection of cell mass due to net growth moved the live and dead cells at the same rate. Live and dead cells were assumed to detach at the biofilm-bulk liquid interface at the same rate. The detachment rate was modeled as being proportional to the square of the biofilm thickness (21, 25).

The interaction of an antibiotic with the biofilm was modeled in two different ways, simulating an explanation for biofilm resistance involving either physiological reduction in susceptibility or antibiotic consumption. In both cases, live cells could be converted to dead cells by the presence of the antibiotic. The importance of physiological gradients was captured in the first case by making the rate of conversion of live to dead cells first order in the antibiotic concentration and directly proportional to the local specific growth rate of the live cells. This second feature incorporates the known growth rate dependence of killing of β-lactam antibiotics (23) and tobramycin (7). For this first case, it was assumed that the antibiotic did not react with system components or biomass. In the second case, the antibiotic was allowed to react with live and dead cells at a rate that was first order in both biomass and antibiotic. The kill rate was made independent of the growth rate in this second case.

Parameter values used in the simulations and their sources are recorded in Table 1. Biofilm thicknesses and biofilm areal cell densities were converted by using an average biofilm cell density ($\varepsilon_c\rho_x$) of 4,700 g of carbon per $m^3$, obtained by review of extensive measurements on *Pseudomonas aeruginosa* biofilms (6, 17, 20). To compare experiment and theory, the data described by Anwar et al. (1) were converted from CFU per centimeter of tubing to CFU per square centimeter by using the surface area of the tubing pieces, which was calculated to be 3.47 $cm^2$/cm. By this conversion, 2-day-old biofilms had an areal cell density of $9.5 \times 10^6$ CFU/$cm^2$ and 7-day-old biofilms had a density of $6.0 \times 10^8$ CFU/$cm^2$.

## RESULTS

A biofilm accumulation model was used to simulate the experimental results described by Anwar et al., in which chemostat-grown *P. aeruginosa* biofilms were treated with a combination of tobramycin and piperacillin. The first simulation involved matching biofilm accumulation data before antibiotic therapy was initiated (Fig. 1). Three parameters were varied to achieve the fit. Each parameter corresponded to information contained in distinct features of the experimental data: the initial biofilm areal cell density, final biofilm areal cell density, and the rate of biofilm accumulation. The initial amount of biofilm, input to the model as a biofilm thickness, was obtained from the areal cell density reported by Anwar et

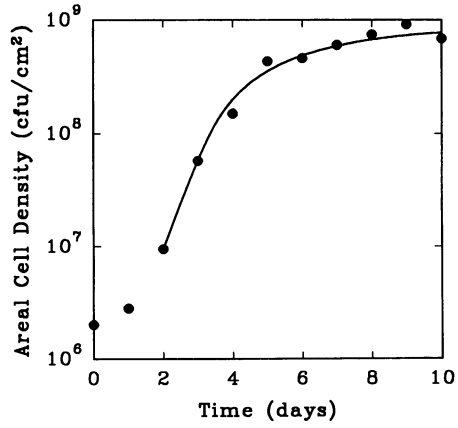


FIG. 1. Biofilm accumulation. ●, data described by Anwar et al.; ——, model fit.

al. for 2-day-old biofilms. The simulation was begun at 2 days because the model could not capture the prior lag phase evident in the data. This simulation spanned the range of biofilm ages investigated experimentally by Anwar et al., since antibiotic treatment was performed on biofilms that were 2 or 7 days old. The rate of biofilm growth was determined by the bulk oxygen concentration, which was adjusted to match the observed biofilm accumulation rate in the interval between 2 and 5 days. The plateau or steady-state amount of biofilm was determined by the detachment coefficient. The result of this fitting process was a good match to the experimental data. Once these three parameters were set by matching the data in Fig. 1, they were left unchanged for all subsequent simulations.

The fitting of the model to a set of data, as reflected in Fig. 1, 3, and 4, was achieved by inspection. That is, one parameter at a time was varied, and the predicted theoretical behavior was compared visually with the experimental data. Once a value of the parameter was found that allowed a reasonable qualitative match of the data, that parameter value was fixed. This approach does not ensure an optimal solution or permit parameter identifiability to be addressed, but it is quite adequate for the purpose of demonstrating the plausibility of a phenomenological concept. It suffices to this end to show that there exists a set of parameter values that provide the same qualitative result exhibited by the experimental data.

The identical model configuration and parameter values that described biofilm accumulation (Fig. 1) also predicted gradients in oxygen concentrations and specific growth rates within the biofilm (Fig. 2). Again, these simulations considered the situation in a growing biofilm before antibiotic treatment. Whereas 2-day-old biofilms exhibited negligible gradients across their 1.4-μm depth, significant gradients were anticipated within 7-day-old, 87-μm-thick biofilms. The depletion of oxygen inside the thicker biofilms restricted the region of rapid bacterial growth to the outer 20 to 30% of the film. There are no data from the study by Anwar et al. with which to evaluate the predictions presented in Fig. 2.

With basic parameters for biofilm accumulation determined, the model was applied to simulate two scenarios of biofilm-antibiotic interaction, as described in Materials and Methods. The results from these two cases, which involved growth rate-dependent killing and antibiotic reaction with the biofilm, respectively, are presented separately below. All of the model runs incorporating antibiotic treatment simulated an 8-h period following addition of the antibiotic to correspond to the interval examined experimentally. Simulations focused on the behavior of 2- and 7-day-old biofilms, facilitating comparison with the experimental results described by Anwar et al. Model outputs of interest for these runs were the local concentration of live cells within the biofilm and the biofilm thickness at the end of the 8-h treatment period.

**Biofilm resistance through growth rate-dependent killing.** To model growth rate-dependent killing of the biofilm, a single additional unknown parameter, the antibiotic specific kill rate, had to be specified. The numerical value of this parameter was determined by matching the data described by Anwar et al. for survival in 2-day-old biofilms (Fig. 3). The data and model fit both indicated a decrease in survival fraction of somewhat greater than 2 log units during 8 h. Without a change in any of the intrinsic parameters, the initial biofilm thickness was raised to 87 μm to simulate the action of an antibiotic on a 7-day-old biofilm. For the 7-day-old biofilm, both the model and the data indicated less than 1 log unit of killing. The model successfully predicted, at least in order of magnitude terms, the relative resistance of the 7-day-old biofilm compared with that of the 2-day-old one. Growth rate-dependent killing was crucial to this difference in this configuration of the model. When the rate of killing was made independent of the growth rate, 2- and 7-day-old biofilms experienced identical decreases in survival fractions (simulation not shown).

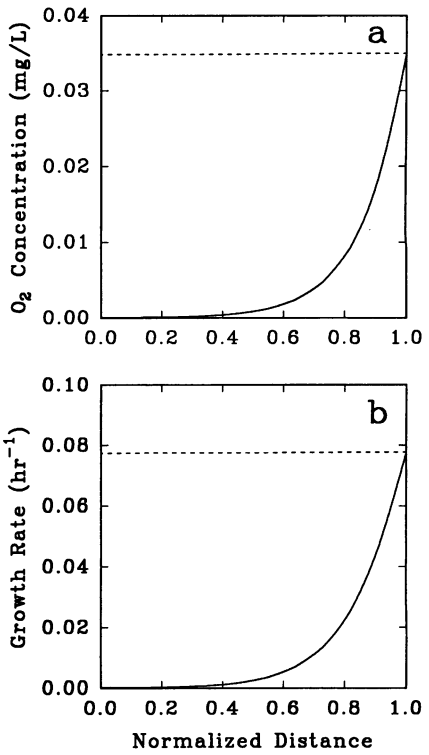


FIG. 2. Theoretical oxygen and specific growth rate profiles within biofilms. The predicted oxygen concentration (a) and specific growth rate (b) are shown for 2-day-old (– –) and 7-day-old (——) biofilms. The $x$ axis is normalized so that $x = 0$ corresponds to the colonized substratum and $x = 1$ corresponds to the biofilm-fluid interface. The dimensional thicknesses of 2- and 7-day-old biofilms were 1.4 and 87 μm, respectively.

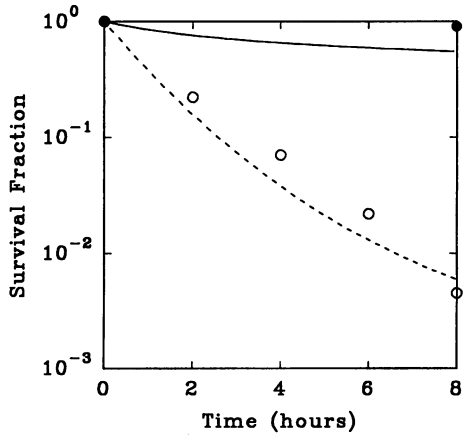


FIG. 3. Survival in antibiotic-treated biofilms; growth rate-dependent killing simulation. Data described by Anwar et al. for treatment of 2-day old biofilm (○) were fit by adjusting the value of the antibiotic kill rate in the model (– –). Without further adjustment, the model was used to predict the behavior of a 7-day-old biofilm (——); data described by Anwar et al. for a 7-day-old biofilm are compared (●).

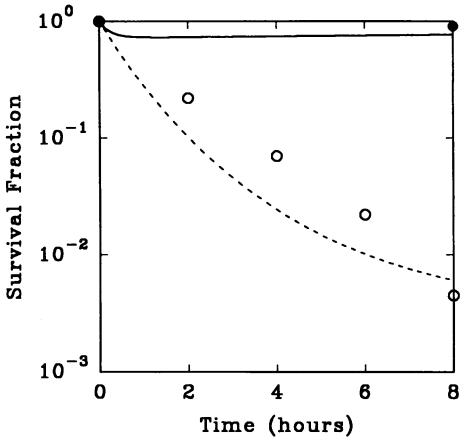


FIG. 4. Survival in antibiotic-treated biofilms; antibiotic reaction with biofilm simulation. Data described by Anwar et al. for treatment of a 2-day-old biofilm (○) were fit by adjusting the value of the antibiotic kill and reaction rates in the model (– –). Without further adjustment, the model was used to predict the behavior of a 7-day-old biofilm (——); data described by Anwar et al. for a 7-day-old biofilm are compared (●).

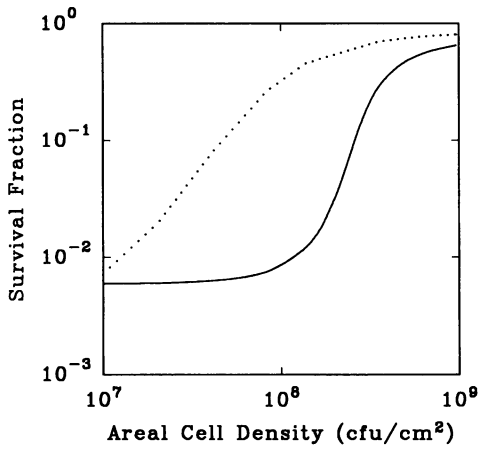


FIG. 5. Predicted effect of biofilm areal density on survival of 8-h treatment with an antibiotic for growth rate-dependent killing (——) and antibiotic reaction with biofilm (. . .) simulations.

**Biofilm resistance through reaction of the antibiotic with the biofilm.** Study of the reaction of the antibiotic with the biofilm examined the possibility that thick biofilms are relatively protected from antibiotics by virtue of consumption of the antimicrobial agent in the biofilm. Two unknown parameters appeared in this problem: the antibiotic kill rate and the antibiotic-cell reaction rate. In contrast to the previous case, the rate of antibiotic killing was made independent of the growth rate for this simulation; thus, the units of the antibiotic kill rate coefficient are different (Table 1). The two parameters were varied to obtain a fit to the data described by Anwar et al. for killing of 2-day-old biofilms (Fig. 4). As with the first case, the model predicted (without adjustment of rate parameters) the relative resistance of the 7-day-old biofilm, which exhibited 79% survival over the 8-h treatment duration. There were not significant gradients in antibiotic concentration within the biofilm (simulation not shown); rather, consumption of the antibiotic caused the bulk concentration of the antibiotic to diminish rapidly.

**Comparison of two resistance mechanisms.** Both biofilm resistance mechanisms, as manifested by the modeling runs discussed above, predicted that biofilm susceptibility to the antibiotic would decrease as the biofilm areal cell density increased (Fig. 5). When the resistance was due to slow growth in thicker biofilms, attached bacteria became sharply more resistant at areal cell densities of greater than about $10^8$ CFU/cm$^2$. Below this threshold, the survival fraction was insensitive to the biofilm cell density. On the other hand, when resistance was due to consumption of the antibiotic, biofilm resistance was approximately proportional to areal cell density at all densities of less than about $10^8$ CFU/cm$^2$. At areal cell densities of greater than $10^8$ CFU/cm$^2$, biofilms in which there was reaction of the antibiotic were very resistant to killing.

The two resistance mechanisms predicted different survival patterns inside thick biofilms (Fig. 6). In the growth rate-dependent killing case, most of the killing occurred in the outer half of the biofilm. Cells in the depth of the biofilm survived in high numbers. At the biofilm surface, the survival fraction was 0.014, whereas at the base of the biofilm, the survival fraction was 0.98. No such steep gradient in survival was observed when biofilm resistance was due to antibiotic depletion through reaction. In this case, cells survived at approximately 75% nearly uniformly across the depth of the biofilm.

## DISCUSSION

A mathematical model of biofilm accumulation was applied to evaluate the plausibility of two proposed mechanisms of biofilm resistance to antibiotics. The mechanisms involved either poor penetration of the antibiotic, due to its consumption by reaction with biomass, or physiological resistance due to reduced bacterial growth rates in the biofilm. Both mechanisms predicted reduced antibiotic susceptibilities of 7-day-old biofilms compared with those of 2-day-old films, as reported by Anwar et al. (1). This modeling study lends credence to both mechanisms (or a combination) as plausible explanations for the reduced susceptibilities of biofilm microorganisms to antimicrobial agents.

A model that incorporated growth rate-dependent killing

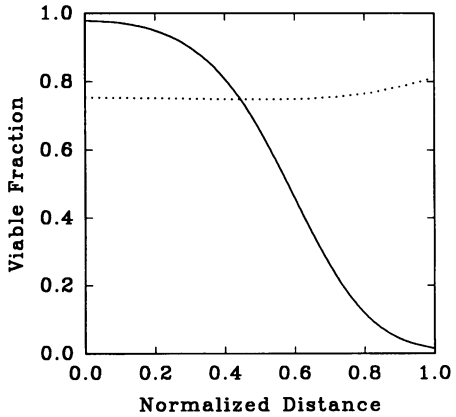


FIG. 6. Survival gradient within antibiotic-treated biofilms. The local viable fraction within 7-day-old biofilms after 8 h of antimicrobial treatment is shown for growth rate-dependent killing (——) and antibiotic reaction with biofilm (. . .) simulations. The $x$ axis is normalized so that $x = 0$ corresponds to the colonized substratum and $x = 1$ corresponds to the biofilm-fluid interface. The dimensional thickness of the biofilm after treatment was 85 μm.

predicted reduced susceptibility of thicker biofilms because oxygen was exhausted within these biofilms, leading to very slow growth in part of the films. In thin (2-day-old) biofilms, oxygen penetrated the biofilms fully (Fig. 2). In these biofilms, there were no regions of slow growth; therefore, the antibiotic was relatively effective. Biofilms that were 7 days old were predicted to suffer severe oxygen limitation in about half of the biofilm, leading to a significant region of retarded growth (Fig. 2). Cells in the slowly growing region survived the antibiotic treatment in high numbers (Fig. 6).

Biofilm resistance was also adequately explained by a model that accounted for depletion of the antibiotic through reaction with biomass. However, this was not because the antibiotic failed to penetrate the biofilm fully. Even with mature, 7-day-old biofilms, there was little gradient in antibiotic concentration across the depth of the biofilm. The resistance in this case was instead due to depletion of the antibiotic in the bulk fluid. In other words, the reaction of the antibiotic with the biomass was slow enough that concentration gradients did not develop inside the biofilm but fast enough that the antibiotic was consumed in the chemostat as a whole. This result underscores the need to consider the biofilm, whether in vitro on in vivo, in the context of a particular reactor or system configuration. Biofilm activity is intimately coupled to and dependent on the geometry (areas and volumes) and flow rates of the larger system.

In Fig. 3 and 4, the model predicts a nonlinear kill curve for 2-day-old biofilms, whereas the experimental data suggest an approximately linear decline. The nonlinear behavior of the model is expected in all cases simply because of the continual dilution of the antibiotic in the chemostat. After 8 h, the bulk concentration of antibiotic should be reduced to 36.8% of its initial value, even in the absence of antibiotic consumption. The model correctly captures the order of magnitude of the observed response. The discrepancy between the shapes of the theoretical and experimental kill curves could be due to imperfect bulk fluid mixing in the chemostat vessel, nonlinear kill kinetics, or inherent variability in the experimental measurements.

Nichols and coworkers mathematically modeled the diffusion of a β-lactam antibiotic into a microbial colony and concluded, in agreement with the present study, that the antimicrobial agent should readily penetrate the biofilm (14, 15). Their work did not consider the depletion of the antibiotic in the fluid surrounding the microcolony and thus did not identify the reaction or binding of the antibiotic as a potential mechanism of resistance. This difference between the conclusions of Nichols's modeling and that reported in the present paper reinforces the importance of the larger geometrical configuration and flow context of the microcolony or biofilm. By way of comparison, the reaction rate constant used in this work was equivalent to a first-order rate constant of $2.1 \times 10^{-3}\ s^{-1}$, a value that is bracketed by the range of β-lactamase hydrolysis coefficients used in one modeling study by Nichols (14).

Particularly with complex systems such as a biofilm, mathematical modeling can aid in the interpretation of data and can guide experimental design. For example, by revealing differences in the behavior predicted by two mechanisms of biofilm resistance, the present study suggests specific experiments that could discriminate them. One quite dramatic difference between the mechanisms is the predicted survival gradient within the biofilm (Fig. 6). Such gradients could possibly be experimentally visualized through the use of physiological stains, for example, for respiratory activity (19) or RNA (13), or by radiolabeling and autoradiography (22). Another difference between the predictions of the two resistance mechanisms is the dependence of survival fraction on areal cell density. Additional experiments at intermediate cell densities, for example, on biofilms between 2 and 7 days old, could be valuable in this regard. Yet another experimental approach suggested by the modeling would be to investigate the reaction of the antibiotic in the reactor over time scales (1 to 4 h) shorter than that used by Anwar et al. On a cautionary note, it must be remembered that the predictions of this investigation are specific to the experimental system used by Anwar et al. They cannot be assumed to generalize.

Models of biofilm and immobilized cell activity have been widely applied by engineers for research and reactor design purposes. However, only in a few instances (5, 14, 15) have mathematical models of biofilm activity been applied to address medical questions. As illustrated in this report, existing biofilm models could be readily adapted to tackle issues of biofilms in medicine. The use of such models has the potential to enhance experimental design and analysis.

## ACKNOWLEDGMENTS

This work was supported by the Center for Biofilm Engineering at Montana State University, a National Science Foundation-supported Engineering Research Center (cooperative agreement ECD-8907039), and by the Center's Industrial Associates.

I thank G. A. McFeters, F. P. Yu, and J. W. Costerton for their review of the manuscript and M. Hamilton for helpful advice regarding model analysis.

## APPENDIX

This appendix presents the full mathematical formulation of the phenomenological model used in this paper. Differential material balances along with their associated initial and boundary conditions constitute the model. Balance equations within the biofilm are coupled to balances on the bulk fluid of the reactor; balances in the two compartments are separated below for clarity.

**Biofilm compartment.** The concentrations of live cells, dead cells, oxygen, and antibiotic inside the biofilm are analyzed. Cell concentrations inside the biofilm are represented in terms of the fraction of all cells. The concentrations of live and dead cells are thus subject to the constraint

$$\varepsilon_a + \varepsilon_i = 1 \tag{1}$$

The balance on live cells is

$$\frac{\partial \varepsilon_a}{\partial t} = \mu \varepsilon_a - \frac{\partial}{\partial z}(v \varepsilon_a) - k_a C_a \varepsilon_a \tag{2}$$

with

$$\varepsilon_a^o = 1 \text{ at } t = 0 \text{ for } 0 \le z \le L_f^o \tag{3}$$

To incorporate growth rate-dependent killing, the last term in equation 2 is replaced with $k_a \mu C_a \varepsilon_a$.

The advective velocity must satisfy

$$\frac{\partial v}{\partial z} = \mu \varepsilon_a \tag{4}$$

subject to the boundary condition

$$v = 0 \text{ at } z = 0 \text{ for } t > 0 \tag{5}$$

The thickness of the biofilm changes according to

$$\frac{dL_f}{dt} = v\big|_{z=L_f} - k_d L_f^2 \tag{6}$$

with

$$L_f = L_f^o \text{ at } t = 0 \tag{7}$$

The concentration of oxygen in the biofilm is described by

$$\frac{\partial C_o}{\partial t} = D_o\tau \frac{\partial^2 C_o}{\partial z^2} - \frac{\mu}{Y_{xo}} \frac{C_o}{K_o + C_o} \varepsilon_a \varepsilon_c \rho_x \quad (8)$$

with the initial condition

$$C_o = C_o^* \text{ at } t = 0 \text{ for } 0 \le z \le L_f^o \quad (9)$$

and boundary conditions imposing the bulk fluid concentration at the biofilm surface

$$C_o = C_o^* \text{ at } z = L_f \text{ for } t \ge 0 \quad (10)$$

and a no flux condition at the substratum

$$\frac{\partial C_o}{\partial z} = 0 \text{ at } z = 0 \text{ for } t \ge 0 \quad (11)$$

The specific growth rate at any point in the biofilm is calculated from the local oxygen concentration according to a Monod dependence

$$\mu = \mu_{max} \frac{C_o}{K_o + C_o} \quad (12)$$

The antibiotic concentration is given by

$$\frac{\partial C_a}{\partial t} = D_a\tau \frac{\partial^2 C_a}{\partial z^2} - k_r C_a \varepsilon_c \varepsilon_a \rho_x \quad (13)$$

with initial and boundary conditions

$$C_a = C_a^* \text{ at } t = 0 \text{ for } 0 \le z \le L_f^o \quad (14)$$

$$C_a = C_a^* \text{ at } z = L_f \text{ for } t > 0 \quad (15)$$

$$\frac{\partial C_a}{\partial z} = 0 \text{ at } z = 0 \text{ for } t > 0 \quad (16)$$

In the case in which no reaction of the antibiotic occurs, the second term in equation 13 is omitted.

**Bulk fluid compartment.** Differential material balances on the bulk fluid compartment account for flow in and out of the chemostat, reaction in the bulk phase, and the net reaction arising from the biofilm. The balances on live and dead cells are

$$\frac{dX_a^*}{dt} = \mu X_a^* + k_d \varepsilon_c \varepsilon_a \big|_{z=L_f} \rho_x L_f^2 \frac{A}{V} - \frac{Q}{V} X_a^* \quad (17)$$

with initial conditions

$$\frac{dX_i^*}{dt} = k_d \varepsilon_c \varepsilon_i \big|_{z=L_f} \rho_x L_f^2 \frac{A}{V} - \frac{Q}{V} X_i^* \quad (18)$$

$$X_a^* = X_i^* = 0 \text{ at } t = 0 \quad (19)$$

The antibiotic concentration in the bulk is given by

$$\frac{dC_a^*}{dt} = -\frac{Q}{V} C_a^* - k_r C_a^* (X_a^* + X_i^*) - D_a\tau \frac{dC_a}{dz} \big|_{z=L_f} \frac{A}{V} \quad (20)$$

with

$$C_a^* = C_a^{*o} \text{ at } t = 0 \quad (21)$$

The bulk concentration of oxygen is fixed.

These equations are solved numerically by a finite-difference method using a tridiagonal technique and a variable time step.

**Nomenclature. (i) Latin characters.** Latin characters are defined as follows: $A$, biofilm surface area; $C_a$, concentration of the antibiotic; $C_o$, concentration of oxygen; $D_a$, diffusion coefficient of the antibiotic in water; $D_o$, diffusion coefficient of oxygen in water; $k_a$, antibiotic kill rate coefficient; $k_d$, detachment rate coefficient; $k_r$, antibiotic reaction rate coefficient; $K_o$, oxygen Monod half-saturation coefficient; $L_f$, biofilm thickness; $Q$, volumetric flow rate; $t$, time; $v$, cell advective velocity; $X_a^*$, bulk concentration of live cells; $X_i^*$, bulk concentration of dead cells; $Y_{xo}$, yield coefficient of biomass on oxygen; $z$, distance coordinate normal to the substratum.

**(ii) Greek characters:** $\varepsilon_a$, live cell fraction; $\varepsilon_c$, cell fraction of total biofilm volume; $\varepsilon_i$, dead cell fraction; $\mu$, local specific growth rate; $\mu_{max}$, maximum specific growth rate; $\rho_x$, cell intrinsic density; $\tau$, biofilm-bulk fluid effective diffusivity ratio.

**(iii) Superscripts:** $^o$, initial value; *, bulk fluid value.

## REFERENCES


1. **Anwar, H., J. L. Strap, and J. W. Costerton.** 1992. Dynamic interactions of biofilms of mucoid *Pseudomonas aeruginosa* with tobramycin and piperacillin. Antimicrob. Agents Chemother. **36:** 1208–1214.
2. **Bailey, J. E., and D. F. Ollis.** 1986. Biochemical engineering fundamentals. McGraw-Hill, New York.
3. **Brown, M. R. W., D. G. Allison, and P. Gilbert.** 1988. Resistance of bacterial biofilms to antibiotics: a growth-rate related effect? J. Antimicrob. Chemother. **22:**777–783.
4. **Costerton, J. W., K.-J. Cheng, G. G. Geesey, T. I. Ladd, J. C. Nickel, M. Dasgupta, and T. J. Marrie.** 1987. Bacterial biofilms in nature and disease. Ann. Rev. Microbiol. **41:**435–464.
5. **Dibdin, G. H.** 1992. A finite-difference computer model of solute diffusion in bacterial films with simultaneous metabolism and chemical reaction. CABIOS **8:**489–500.
6. **Drury, W. J.** 1992. Interactions of 1-μm latex microbeads with biofilms. Ph.D. thesis. Montana State University, Bozeman, Mont.
7. **Evans, D. J., M. R. W. Brown, D. G. Allison, and P. Gilbert.** 1990. Susceptibility of bacterial biofilms to tobramycin: role of specific growth rate and phase in division cycle. J. Antimicrob. Chemother. **25:**585–591.
8. **Gilbert, P., P. J. Collier, and M. R. W. Brown.** 1990. Influence of growth rate on susceptibility to antimicrobial agents: biofilms, cell cycle, dormancy, and stringent response. Antimicrob. Agents Chemother. **34:**1865–1868.
9. **Goldstein, B. R., and M. A. Hamilton.** Submitted for publication.
10. **Hoyle, B. D., and J. W. Costerton.** 1991. Bacterial resistance to antibiotics: the role of biofilms. Prog. Drug Res. **37:**91–105.
11. **Leitão, J. H., A. M. Fialho, and I. Sá-Correia.** 1992. Effects of growth temperature on alginate synthesis and enzymes in *Pseudomonas aeruginosa* variants. J. Gen. Microbiol. **138:**605–610.
12. **Lewandowski, Z., G. Walser, and W. G. Characklis.** 1991. Reaction kinetics in biofilms. Biotechnol. Bioeng. **38:**877–882.
13. **Monbouquette, H. G., G. D. Sayles, and D. F. Ollis.** 1990. Immobilized cell biocatalyst activation and pseudo-stead-state behavior: model and experiment. Biotechnol. Bioeng. **35:**609–629.
14. **Nichols, W. W.** 1989. Susceptibility of biofilms to toxic compounds, p. 321–332. *In* P. A. Wilderer and W. G. Characklis (ed.), Structure and function of biofilms, Wiley Interscience, New York.
15. **Nichols, W. W., M. J. Evans, M. P. E. Slack, and H. L. Walmsley.** 1989. The penetration of antibiotics into aggregates of mucoid and nonmucoid *Pseudomonas aeruginosa*. J. Gen. Microbiol. **135:**1291–1303.
16. **Perry, R. H., and C. H. Chilton.** 1973. Chemical engineer's handbook, 5th ed. McGraw-Hill, New York.
17. **Peyton, B. M.** 1992. Ph.D. thesis. Montana State University, Bozeman, Mont.
18. **Robinson, J. A., M. G. Trulear, and W. G. Characklis.** 1984. Cellular reproduction and extracellular polymer formation by *Pseudomonas aeruginosa* in continuous culture. Biotechnol. Bioeng. **26:**1409–1417.
19. **Rodriguez, G. G., D. Phipps, K. Ishiguro, and H. F. Ridgway.** 1992. Use of a fluorescent redox probe for direct visualization of actively respiring bacteria. Appl. Environ. Microbiol. **58:**1801–1808.
20. **Siebel, M. A.** 1987. Binary population biofilms. Ph.D. thesis. Montana State University, Bozeman, Mont.
21. **Stewart, P. S.** 1993. A model of biofilm detachment. Biotechnol. Bioeng. **41:**111–117.
22. **Stewart, P. S., S. F. Karel, and C. R. Robertson.** 1991. Characterization of immobilized cell growth rates using autoradiography.

Biotechnol. Bioeng. **37:**824–833.
23. **Tuomanen, E., R. Cozens, W. Tosch, O. Zak, and A. Tomasz.** 1986. The rate of killing of *Escherichia coli* by β-lactam antibiotics is strictly proportional to the rate of bacterial growth. J. Gen. Microbiol. **132:**1297–1304.
24. **Turakhia, M. H., and W. G. Characklis.** 1989. Activity of *Pseudomonas aeruginosa* in biofilms: effect of calcium. Biotechnol. Bioeng. **33:**406–414.
25. **Wanner, O., and W. Gujer.** 1986. A multispecies biofilm model. Biotechnol. Bioeng. **28:**314–328.
26. **Westrin, B. A., and A. Axelsson.** 1991. Diffusion in gels containing immobilized cells: a critical review. Biotechnol. Bioeng. **38:**439–446.